JACS
JOURNAL OF THE AMERICAN CHEMICAL SOCIETY

ARTICLE

pubs.acs.org/JACS

# Ions in Size-Selected Aqueous Nanodrops: Sequential Water Molecule Binding Energies and Effects of Water on Ion Fluorescence

William A. Donald,[§] Ryan D. Leib,[⊥] Maria Demireva, and Evan R. Williams*

Department of Chemistry, University of California, Berkeley, California, 94720-1460

**ABSTRACT:** The effects of water on ion fluorescence were investigated, and average sequential water molecule binding energies to hydrated ions, $M^z(H_2O)_n$, at large cluster size were measured using ion nanocalorimetry. Upon 248-nm excitation, nanodrops with ~25 or more water molecules that contain either rhodamine $590^+$, rhodamine $640^+$, or $Ce^{3+}$ emit a photon with average energies of approximately 548, 590, and 348 nm, respectively. These values are very close to the emission maxima of the corresponding ions in solution, indicating that the photophysical properties of these ions in the nanodrops approach those of the fully hydrated ions at relatively small cluster size. As occurs in solution, these ions in nanodrops with 8 or more water molecules fluoresce with a quantum yield of ~1. $Ce^{3+}$ containing nanodrops that also contain $OH^-$ fluoresce, whereas those with $NO_3^-$ do not. This indirect fluorescence detection method has the advantages of high sensitivity, and both the size of the nanodrops as well as their constituents can be carefully controlled. For ions that do not fluoresce in solution, such as protonated tryptophan, full internal conversion of the absorbed 248-nm photon occurs, and the average sequential water molecule binding energies to the hydrated ions can be accurately obtained at large cluster sizes. The average sequential water molecule binding energies for $TrpH^+(H_2O)_n$ and a doubly protonated tripeptide, $[KYK + 2H]^{2+}(H_2O)_n$, approach asymptotic values of ~9.3 ($n \geq 11$) and ~10.0 kcal/mol ($n \geq 25$), respectively, consistent with a liquidlike structure of water in these nanodrops.

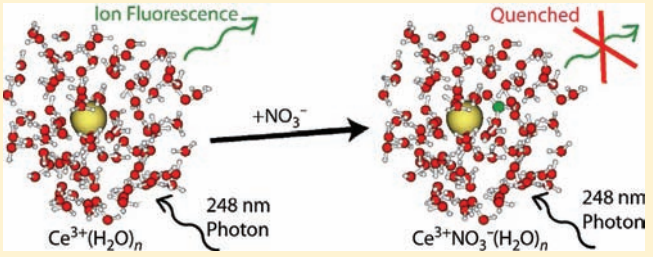


## INTRODUCTION

Solvent plays a pivotal role in the structures, dynamics, and functions of many molecules and ions.[1] Water is ubiquitous in nature and is arguably the most important solvent,[2] yet much remains unknown about how water molecules interact with ions and molecules and how ions can affect the hydrogen-bonding interactions of water itself. Water molecules can form strong interactions with proteins and can be vital to protein structure and reactivity, whereas some water molecules, such as those at the protein surface, may interact only slightly more strongly with the protein than with other water molecules.[3] Water stabilizes ionic interactions and can dramatically affect acid−base chemistry. For example, *p*-aminobenzoic acid is protonated at the amino group in water,[4] but protonation at the carboxylic acid site is more favorable in the gas phase.[5] However, salt bridges between basic and acidic sites, which are important for protein structure in solution, can exist in the gas phase even when there is no solvent or significant intramolecular solvation to stabilize these ionic interactions.[6] By comparing structures and reactivities of ions and molecules in the gas phase to those in aqueous solution, the role of water on molecular structure and energetics can be inferred. The growing use of mass spectrometry to investigate the structures of specific macromolecular complexes using gas-phase structural probes, such as ion mobility spectrometry,[7] has resulted in an increased interest in developing complementary methods that could potentially be used to obtain even more detailed structural information.

In the condensed phase, laser-induced fluorescence is widely used as a sensitive detection method, and through Förster resonance energy transfer (FRET) measurements, information about both structure and dynamics of large molecules can be obtained.[8] In contrast, fluorescence detection of trapped ions in the gas phase is significantly less common largely owing to the experimental challenges of efficiently collecting photons that are emitted isotropically from a small number of ions confined within an ion-trapping device and background due to scattering. Laser-induced fluorescence has been measured for a number of relatively small ions[9] and for dye-tagged biomolecules in ion-trapping devices,[10] and FRET in trapped and unsolvated gaseous ions has been reported.[9a,10a,10b] In pioneering experiments by Parks and co-workers,[10a] the gas-phase dissociation dynamics of a double-stranded dye-tagged oligonucleotide complex ion was investigated by monitoring the change in the FRET intensity. By extending such measurements to ions with a controlled number of solvent molecules attached, detailed information about how solvent affects the structures and excited-state dynamics of biomolecules could potentially be obtained. However, the direct detection of fluorescence by partially hydrated gaseous ions has not yet been achieved.

Recently, we introduced a new method for indirectly detecting the fluorescence of hydrated gas-phase ions using ion nanocalorimetry.[11]

**Received:** August 26, 2011
**Published:** October 14, 2011

**Chart 1. Structures of (a) Protonated Proflavine, (b) Rhodamine 590, (c) Rhodamine 640, and (d) Paraquat**

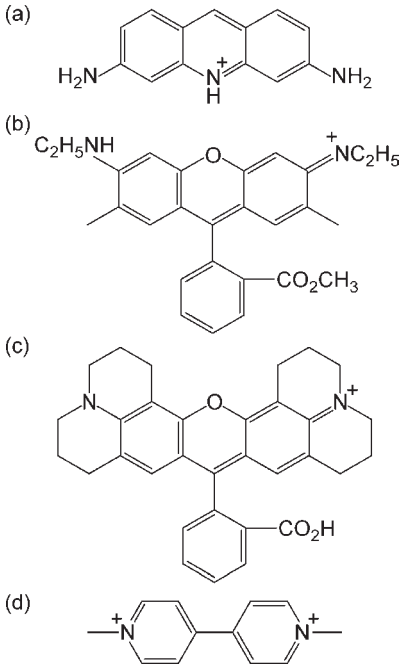


In this method, a size-selected partially hydrated ion, $M^z(H_2O)_n$, where $M^z$ is an ion with charge $z$, is isolated and subjected to one of a variety of ion-activation techniques, such as electron capture[12] or ultraviolet (UV) photodissociation.[11,13] Electronic excitation of these isolated 'nanodrops' typically results in the rapid conversion of electronic to internal energy, cluster heating, and the liberation of water molecules from the activated cluster through evaporative cooling. The extent of the energy deposited into the precursor ion is determined from the number of water molecules lost from the cluster. However, if an electronically excited ion fluoresces,[11] then the internal energy available for evaporating water molecules from the cluster is reduced by the energy corresponding to the emitted photon, and thus fewer water molecules are lost. The energy of the emitted photon is equal to the difference in the energy of the absorbed photon and the energy removed by the water molecules that are lost from the cluster ion that has fluoresced.[11] Thus, the fluorescence of a hydrated ion can be *indirectly* detected by measuring a laser-induced photodissociation mass spectrum of the hydrated fluorophore ion. No optics for the direct collection and detection of fluorescent photons are required. A key advantage of this approach is that all dissociation products resulting from photon emission are measured irrespective of the direction in which the photons are emitted. This is equivalent to collecting 100% of the emitted photons using more traditional fluorescence detection methods, which makes this indirect method for detecting ion fluorescence very sensitive. Accurate fluorescence quantum yields, which are the fraction of ions that emit a fluorescent photon upon absorption of an excitation photon, can also be readily obtained.[11]

This new indirect fluorescence detection method was first demonstrated with hydrated protonated proflavine, $PH^+(H_2O)_n(g)$, $n$ = 13−50 (see Chart 1).[11] Upon absorption of a 248-nm photon, two resolved product ion distributions are formed at large $n$ corresponding to the loss of ∼6 water molecules for ions that fluoresced or to the loss of ∼11 water molecules for full internal conversion of the photon energy. The energy of the emitted photon was obtained from the number of water molecules lost to form each respective distribution, and the fluorescence quantum yield was obtained from the relative abundances of the respective distributions. The energy of the emitted photon red-shifted from ∼450 to 580 nm with increasing cluster size and approached the onset of $PH^+$ fluorescence in the condensed phase (600 nm). The fluorescence quantum yield of $PH^+(H_2O)_n(g)$, for $n \geq 32$, is the same as the bulk fluorescence quantum yield, and this value increases rapidly with decreasing cluster size, consistent with less efficient conversion of electronic-to-vibrational energy for clusters with fewer water molecules. These results indicate that only a relatively small number of water molecules (about 30) are required to make these excited-state properties of partially hydrated $PH^+$ approach those of $PH^+(aq)$. Other results indicate that nanodrops containing water molecules in the second or higher solvation shells can exhibit other properties similar to those of bulk, such as redox properties,[12a−c] hydrolysis reactivity,[12d,14] ion coordination numbers,[15] and structure of the water network.[16]

For cases in which absorption of a visible or UV photon by a hydrated ion results in full internal conversion of the photon energy,[13] the sequential water molecule binding enthalpies to the cluster can be obtained from the number of water molecules lost and from the energy that partitions into translations, rotations, and vibrations ($E_{TRV}$) for each water molecule that is lost. This method of obtaining sequential water molecule binding enthalpies has the advantage that the fundamental interactions between ions and water molecules can be investigated well past three solvation shells[13] and with comparable accuracy to more traditional thermochemical methods[17] for obtaining binding energies and enthalpies for much smaller clusters. Thus, information about the excited state of the partially hydrated ion and the strength of the interactions between the ion and the solvent molecules can be obtained from a single photodissociation experiment. The sequential binding enthalpies and entropies of water molecules to small protonated biomolecules[18] have been measured for small extents of hydration ($n < 6$) using equilibrium mass spectrometry. However, much less is known about the strength of water−ion interactions in larger clusters, which contain water molecules in the second or higher solvation shells.

Here, we report UV photodissociation experiments on size-selected nanodrops, $M^z(H_2O)_n$, for a variety of fluorescent and nonfluorescent ions. From these results, information is obtained about how water directly affects the fluorescence of molecular ions, the strength of water−ion interactions at large ion hydration extents, and how the physical properties of ions progress toward those of the fully solvated ion.

## METHODS

**Experiments.** A home-built 2.75 T Fourier transform ion cyclotron resonance (FT/ICR) mass spectrometer equipped with an external nanoelectrospray (nESI) ion source[19] and a temperature-controlled ion cell was used for all experiments.[17a] Extensively hydrated ions were formed from ∼1 mM aqueous solutions containing the ions of interest. A potential of ∼500 V relative to the heated capillary entrance (∼40−100 °C) of the mass spectrometer was applied to a Pt wire that was in direct contact with the nESI solution contained in a pulled borosilicate capillary (inner tip diameter of ∼1−2 μm). Ions were

transferred through five stages of differential pumping and were accumulated for 3 s in the ion cell of the FT/ICR mass spectrometer. During ion accumulation, dry $N_2$(g) was pulsed into the vacuum chamber surrounding the ion cell to a pressure of $\sim 10^{-6}$ Torr to enhance trapping and thermalization of the ions. Additional ions were prevented from entering the ion cell both before and after ion accumulation by a mechanical shutter that is only open during ion accumulation. A delay of 4 s after ion accumulation ensures that the pressure of the vacuum chamber surrounding the ion cell returns to $<10^{-8}$ Torr and that the ions have steady-state internal energy distributions. The Cu jacket surrounding the ion cell was equilibrated to 133 K overnight prior to data acquisition.

For UV photodissociation experiments,[11,13] including indirect fluorescence detection experiments,[11] ions were isolated using SWIFT techniques. After a delay of 50 ms, a mechanical shutter controlled by a rotary solenoid was opened, and 248-nm light (4.991 ± 0.004 eV; 8 W) from an excimer laser (EX100, GAM Laser Co., FL, U.S.A.) was focused through a 1-m focal length $CaF_2$ lens placed ~1.25 m from the ion cell center. The light enters the vacuum chamber through a $CaF_2$ ultrahigh-vacuum compatible window. After irradiating the ions for 250 ms, the mechanical shutter was closed to prevent additional laser light from entering the ion cell during ion detection. This ion activation time was chosen as a compromise between increasing the laser-induced dissociation efficiency (via longer irradiation times) and minimizing the amount of precursor ion dissociation resulting from the absorption of blackbody photons from the surrounding vacuum chamber and ion cell (via shorter irradiation times). Precursor and product ions were detected simultaneously after a 50-ms delay between the end of ion irradiation and start of ion detection. This delay ensures that the ions have sufficient time to completely dissociate prior to detection.[13]

The average number of water molecules lost as a result of the absorption of the UV photon, $\langle x \rangle$, was obtained from the difference in the average sizes of the precursor, $\langle n \rangle_b$, and product ion distributions, $\langle p \rangle_b$, at the end of ion irradiation. This method, which has been discussed in detail elsewhere,[13] accounts for the minor amount of dissociation resulting from the absorption of blackbody photons. Values for the average number of water molecules lost are highly reproducible. For example, absorption of a 248-nm photon by $PH^+(H_2O)_{12}$, results in the loss of an average of 5.97 ± 0.02 and 5.93 ± 0.02 water molecules when measured on different days.

**Calculations.** For hydrated ions that fluoresce, the average energy of the emitted photon is obtained from the difference in the average energy removed by the lost water molecules and the energy of the absorbed photon (5.0 eV).[11] The energy removed by the lost water molecules is equal to the sum of the binding energies of the lost water molecules and the $E_{TRV}$ values for each lost water molecule. Sequential water molecule binding energies have not been measured for positively charged rhodamine 590 and 640 ($Rh590^+$ and $Rh640^+$, respectively; see Chart 1), $CeOH^{2+}$, and $Ce^{3+}$. For the two laser dyes, $Rh590^+$ and $Rh640^+$, a value of 9.3 kcal/mol is used as an estimate of the sequential water molecule binding energies to these ions. This value is chosen because the sequential binding energy to protonated tryptophan, $TrpH^+$, at large cluster sizes ($n > 20$) was measured to be ~9.3 kcal/mol (vide infra) and the sequential water molecule binding energies to tetramethyl ammonium, an ion that does not bind water strongly, for $n$ = 1 and 2 are very close to this value, indicating that the sequential water molecule binding energies to the laser dyes should also be largely determined by water−water, as opposed to water−ion, interactions. For $Ce^{3+}$ and $CeOH^{2+}$, the average sequential binding energies are obtained from the Thomson liquid drop model.[20] The $E_{TRV}$ values for each water molecule that is lost are obtained from the Klots' cluster evaporation model[21] as described elsewhere.[12c,e] For $Ce^{3+}$- and $CeOH^{2+}$-containing water clusters, average internal energy values are obtained using harmonic frequencies calculated for an energy-minimized $Ca(H_2O)_{14}^{2+}$ structure and were scaled by the number of vibrational degrees of freedom of the cluster of interest. For the laser dyes, vibrational frequencies were obtained from an energy-optimized OPLS-2005 structure of the respective dye with 20 water molecules and were weighted by the number of vibrational degrees of freedom of the cluster of interest. The structure used was obtained from extensive Monte Carlo conformational searching using Macromodel and the OPLS-2005 force field. Similar calculations using the MMFFs force field resulted in essentially the same emitted photon energies, indicating that the average internal energies of the water clusters are not very sensitive to the specific frequencies used in these calculations.

For ions in which absorption of a 248-nm photon results in full conversion of the photon energy into internal modes of the cluster, average sequential water molecule binding enthalpies for all the water molecules lost from the cluster are obtained from the average number of water molecules lost, the photon energy, and $E_{TRV}$ values for each of the lost water molecules.[13] Assuming that all of the photon energy is instantaneously converted into internal vibrational modes and completely randomized prior to water molecule evaporation, the internal energy of the precursor cluster upon absorption of the 248-nm photon (5.0 eV) is given by[13]

$$U_{i=0}(T^*_{i=0}) = U_P(133\ \mathrm{K}) + 5.0\ \mathrm{eV} \quad (1)$$

where $U_P$(133 K) is the internal energy of the precursor cluster thermalized to a temperature of 133 K, the subscript $i$ designates the cluster identity by how many water molecules have evaporated from the precursor cluster ($i$ = 0) to form this cluster, and 5.0 eV is the energy of the absorbed photon. For each water molecule that is lost, the internal energy of the $i$th cluster is given by

$$U_i(T^*_i) = U_{i-1}(T^*_{i-1}) + \langle E_{n,n-1} \rangle + (5/2)kT^*_{i-1} \quad (2)$$

where $U_i$ is the internal energy of the $i$th cluster, $\langle E_{n,n-1} \rangle$ is the average sequential water molecule binding energy that is an unknown, and $(5/2)kT^*_{i-1}$ is the average $E_{TRV}$ for each water molecule that is lost, which is obtained from Klots' cluster evaporation model,[21] where $T^*_{i-1}$ is the effective temperature of the $(i-1)$ cluster and $k$ is the Boltzmann constant. Under these conditions, vibrational modes of the lost water molecules should not be significantly populated, and energy partitioning into vibrational modes of the lost water molecules should be negligible. Average internal energy values are obtained from a B3LYP/6-311++G** energy-minimized structure of $TrpH^+(H_2O)_5$[18a] and scaled by the vibrational degrees of freedom of the cluster of interest. The system of equations obtained from eqs 1 and 2 results in the same number of equations as unknowns ($\langle E_{n,n-1} \rangle$ and $T^*$ values) and can be solved to obtain values for $T^*$ and $\langle E_{n,n-1} \rangle$. The average sequential water molecule binding enthalpy for each water molecule lost is obtained from eq 3, where the vibrational energy lost upon water molecule loss is approximated as being equal to the gained $E_{TRV}$ of the products ($kT$ = 0.6 kcal/mol at 298 K).

$$\Delta H_{n,n-1} = E_{n,n-1} + kT \quad (3)$$

## RESULTS AND DISCUSSION

**Indirect Detection of Laser-Induced Fluorescence using Mass Spectrometry.** Large ion-containing water clusters are formed from aqueous solutions using electrospray ionization. A single-sized cluster, $M^z(H_2O)_n$, is isolated from the distribution of other ionic water clusters that are formed, trapped, and subjected to 248-nm laser radiation from an excimer laser source. Absorption of a UV photon by the mass-selected cluster can result in full internal conversion (quantum yield = 0), 100%

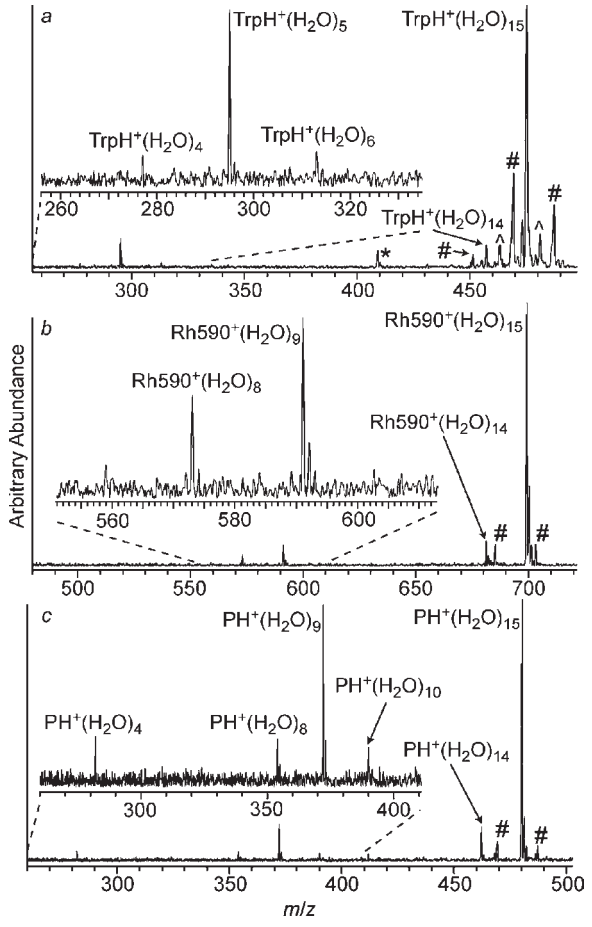


**Figure 1.** Photodissociation (248-nm laser radiation) mass spectrum of $TrpH^+(H_2O)_{15}$, $Rh590^+(H_2O)_{15}$, and $PH^+(H_2O)_{15}$ (250 ms irradiation and 50 ms delay before detection). Insets are vertical and horizontal expansions of the product ion $m/z$ region of the mass spectra. Electronic noise is indicated by ∗ symbols. Peaks corresponding to protonated water clusters (#) and an unknown hydrated monovalent ion series (^) that were not ejected during precursor isolation are indicated.

fluorescence (quantum yield = 1), or competing fluorescence and full internal conversion (0 < quantum yield < 1). Representative photodissociation mass spectra resulting from irradiating the size-selected and thermalized $M^z(H_2O)_{15}$, M = protonated tryptophan ($TrpH^+$; top panel), rhodamine 590 ($Rh590^+$; middle panel), and protonated proflavine ($PH^+$; bottom panel), at 248 nm for 250 ms, which illustrate these three possibilities, are shown in Figure 1.

Upon absorption of a 248-nm photon, $TrpH^+(H_2O)_{15}$ loses 9, 10, and 11 water molecules, corresponding to the formation of $TrpH^+(H_2O)_n$, $n$ = 6, 5, and 4. These product ions are not formed when the laser beam is blocked, whereas the product ion corresponding to the loss of one water molecule from each of the precursor ions is due to its formation by blackbody infrared radiative dissociation (BIRD). The average number of water molecules lost due to the absorption of the 5.0 eV photon (248 nm), $\langle x \rangle$, is obtained from the difference in the average precursor cluster size ($\langle n \rangle_f$) and average product ion cluster size ($\langle p \rangle_f$) at the end of ion irradiation; that is, $\langle x \rangle = 14.92 - 5.02 = 9.90 \pm 0.02$. To the extent that the dissociation resulting from the absorption of blackbody photons by the precursor and product ions during the 50−300 ms between absorption of a 248 nm photon and ion detection is similar, the value of $\langle x \rangle$ should result nearly exclusively from the absorption of the 248 photon; i.e., these values are corrected for BIRD. For $TrpH^+(H_2O)_{15}$, the average energy removed by each of the lost water molecules upon absorption of the 248 nm photon is (5.0 eV)/(9.9 water molecules) = 0.51 eV. This latter value is close to the average sequential water molecule binding energies of large hydrated ions (∼0.4 eV),[13,20] indicating that the energy of the absorbed photon is completely converted into vibrational energy of the precursor ion. The average energy removed by the lost water molecules is somewhat higher than the sequential water molecule binding energies (∼0.4 eV) because each lost water molecule removes some additional energy in the form of translational and rotational energy.

By contrast, $Rh590^+(H_2O)_{15}$ loses only 6 and 7 water molecules upon absorption of a 248-nm photon (Figure 1b). Thus, $Rh590^+(H_2O)_{15}$ loses an average of 3.6 *fewer* water molecules than $TrpH^+$. These data indicate that upon absorption of a 248-nm photon, the partially solvated $Rh590^+$ emits a photon from a higher electronic excited state that is significantly lower in energy than the energy of the absorbed photon, i.e., fluorescence. The remaining electronic energy that is not lost by emission of the photon is converted into vibrational energy of the cluster, resulting in cluster heating and the evaporation of water molecules. The difference in the energy of the absorbed photon (5.0 eV) and the energy removed by the lost water molecules (corresponding to an average of 6.3 water molecules lost) is equal to the energy of the emitted photon. That is, the number of water molecules lost from the cluster is less than if all the energy is converted into vibrational energy of the precursor by an amount corresponding to the energy of the emitted photon. For $Rh590^+(H_2O)_{15}$, a product ion distribution that corresponds to the full internal conversion of the 248-nm photon (i.e., corresponding to the loss of ∼10 water molecules) is not observed, indicating that for every photon that is absorbed, essentially all of the excited ions emit a photon. This indicates that the quantum yield for fluorescence of $Rh590^+(H_2O)_{15}$ is ∼1, which is consistent with the very high quantum yield of $Rh590^+$ in solution that is near unity.[22]

In contrast to the results for the $TrpH^+$- and $Rh590^+$-containing clusters where only a single distribution of lost water molecules is observed, laser-induced excitation of water clusters that contain $PH^+$ at 248 nm results in two product ion distributions.[11] For example, absorption of a 248-nm photon by $PH^+(H_2O)_{15}$ results in a product distribution corresponding to the loss of 5, 6, and 7 water molecules, in addition to the loss of 11 water molecules (Figure 1c). The former distribution results from partial internal conversion of the absorbed photon energy, and either ion fluorescence to relax back to the ground electronic state or intersystem crossing to form a long-lived electronic excited triplet state. The loss of 11 water molecules results from full internal conversion of the photon energy into vibrational energy of the ion. More water molecules are lost from $PH^+(H_2O)_{15}$ upon full internal conversion of the photon than for $TrpH^+(H_2O)_{15}$ likely because the sequential binding energies of water molecules to $TrpH^+$ are slightly higher than for $PH^+$ ($n \leq 15$), which is consistent with the larger size of $PH^+$ and the greater apparent hydrophobicity of this ion, both of which should result in lower sequential water molecule binding energies for $PH^+$ than $TrpH^+$. Because the various photophysical processes for $PH^+(H_2O)_n$ have been described earlier,[11] we will not focus on protonated proflavine further here.

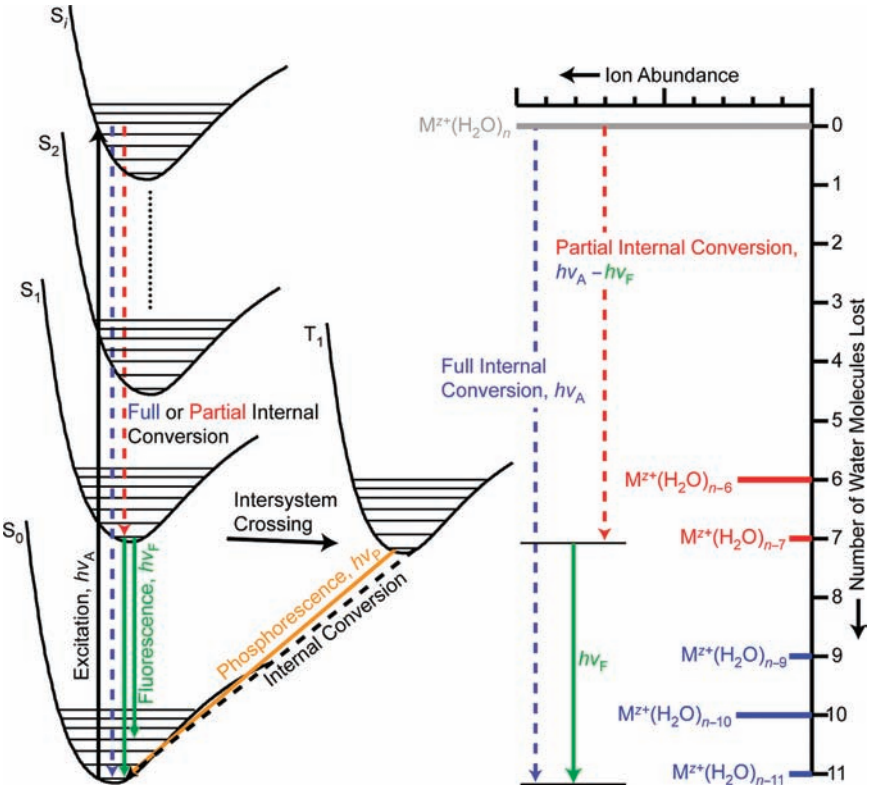


**Figure 2.** Jablonski diagram (left panel) of various photophysical processes that can occur upon electronic excitation of molecules and ions and how such processes can be indirectly detected in mass spectrometry experiments for ionic water clusters (right panel).

**Relation Between Photophysical Processes and Extent of Internal Energy Deposition.** Examples of various photophysical processes that can occur in UV and visible laser excitation experiments are shown in Figure 2 (left). Absorption of a UV or visible photon ($h\nu_A$) by cluster ion in a ground singlet state ($S_0$) at a given starting temperature can result in electronic excitation to a higher electronically excited singlet state ($S_i$). The electronically excited ion can relax back to the ground $S_0$ state and initial temperature by several different photophysical processes. The electronic energy can be completely converted into vibrational energy of the ion, resulting in the heating of the precursor cluster by an amount corresponding to the energy of the absorbed photon. Illustrated in Figure 2 (right) is full internal conversion of the energy of the absorbed photon corresponding to the loss of 9, 10, and 11 water molecules.

Alternatively, photon emission can occur along with only partial internal conversion of the energy of the absorbed photon. In accord with the Kasha−Vavilov rule, fluorescence generally results from a radiative transition between the first singlet electronic excited state and the ground electronic state ($S_1 \leftarrow S_0$).[23] This rule results from both the tendency of polyatomic molecules to have a large $S_1/S_0$ energy gap relative to successive electronic energy states at higher energies and because the rate constants for nonradiative relaxation decrease exponentially as the energy difference between two electronic states increases.[23] Because the rate of internal conversion is generally much faster than fluorescence from higher-energy states, which are closely spaced, the ion will tend to partially relax to the lowest electronic excited state ($S_1$) nonradiatively. Because of the large energy gap between the $S_1$ and $S_0$ state, full relaxation to the $S_0$ state via fluorescence from $S_1$ will be more competitive with internal conversion than fluorescence to $S_0$ from the higher-energy singlet states. Thus, fluorescence generally occurs from the lowest electronically excited singlet state, and fluorescence quantum yields are usually independent of the excitation wavelength for photon energies greater than that corresponding to the $S_1 \leftarrow S_0$ transition. If fluorescence occurs, only part of the energy of the absorbed photon is converted into the internal vibrational energy of the cluster. The energy deposited into the internal modes of the cluster corresponds to the difference between the energy of the absorbed photon ($h\nu_A$) and the energy of the photon that is emitted via fluorescence ($h\nu_F$) (Figure 2, right). Thus, because less energy is deposited into the internal vibrational modes of the precursor cluster when fluorescence occurs, fewer water molecules evaporate from the cluster. In Figure 2, the energy of the photon that is emitted via fluorescence corresponds to the energy required to "boil off" ~4 water molecules from the cluster.

Alternatively, the $S_1$ state can undergo intersystem crossing to form an excited triplet state ($T_1$), which tend to be longer lived species than excited singlet states because relaxation to the ground $S_0$ state, either nonradiatively through the conversion of electronic-to-vibrational energy, or via emission of a photon (via phosphorescence), is a spin-forbidden transition that involves a spin-flip. If intersystem crossing to form a long-lived triplet state occurs, nonradiative intersystem crossing to $S_0$ would result in the conversion of the remaining electronic energy into internal vibrational energy, which will occur in the population over the lifetime of the triplet state. This will result in additional water molecules being lost from the triplet state population. For $PH^+(H_2O)_{50}$, about a third of the population that absorbs a 248 nm photon form a triplet state with a half-life


dx.doi.org/10.1021/ja208072z |J. Am. Chem. Soc. 2011, 133, 18940–18949

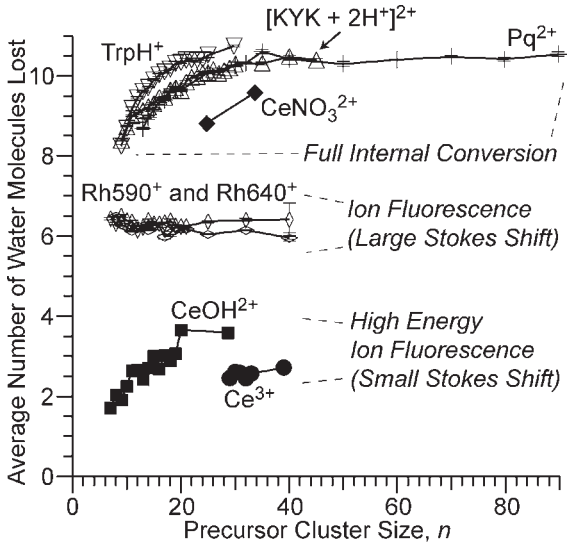


**Figure 3.** Average number of water molecules lost from $M^z(H_2O)_n$, for $M^z$ = $TrpH^+$, $[KYK + 2H^+]^{2+}$, $Pq^{2+}$, $Rh590^+$, $Rh640^+$, $Ce^{3+}$, $CeOH^{2+}$ and $CeNO_3^{2+}$ upon 248 nm photodissociation as a result of absorption of a single 248 nm photon. Error bars represent ±1 standard deviation in these values and are obtained by propagating the noise in the individual mass spectra.

of ~0.5 $s^{-1}$ that undergoes a nonradiative transition to the $S_0$ state.[11] The $T_1/S_0$ energy gap can be determined from the number of water molecules lost if the water clusters containing the long-lived excited fluorophore in the $T_1$ state are given sufficient time to nonradiatively relax to the ground $S_0$ state. Phosphorescence would result in little or no additional water molecules being lost from the triplet state, because the energy would be predominantly removed from the cluster radiatively. Population of a vibrationally excited $S_0$ state resulting from a radiative transition may also contribute slightly to the number of water molecules lost by an amount corresponding to the energy difference between the vibrationally excited $S_0$ state that is formed in the radiative transition and the energy of the thermalized $S_0$ state.

**Effects of Ion Identity.** To investigate the effects of ion identity and cluster size on hydrated ion fluorescence, the average number of water molecules lost as a result of the absorption of a 248 nm photon was measured as a function of cluster size and these data are shown in Figure 3. The photophysics of the various types of ions can be classified into three categories. The first category consists of ions that do not fluoresce upon absorption of the 248 nm photon, and where all of the energy of the absorbed photon goes into evaporating water molecules, which occurs for hydrated $TrpH^+$, a doubly protonated tripeptide ($[KYK+2H^+]^{2+}$), paraquat ($Pq^{2+}$; see Chart 1), and $CeNO_3^{2+}$. The second category includes the hydrated laser dyes, $Rh590^+$ and $Rh640^+$, that emit a photon corresponding to the loss of ~4 fewer water molecules, in which a large Stokes shift occurs, i.e., the emitted photon energy is much lower in energy than the absorbed photon energy. The third category includes hydrated $CeOH^{2+}$ and $Ce^{3+}$, which lose a very small number of water molecules, indicating that the photon that is emitted via fluorescence is only slightly lower in energy than that of the absorbed photon, i.e., a small Stokes shift. The fluorescence quantum efficiencies for hydrated $Rh590^+$, $Rh640^+$, $CeOH^{2+}$, and $Ce^{3+}$ clusters are all essentially 1, which is in excellent agreement with the quantum yields for $Rh590^+$, $Rh640^+$, and $Ce^{3+}$ that are near unity in the condensed phase.[22,24] Data for the fluorescence of $CeOH^{2+}$ (aq) is not available to our knowledge. In contrast, $Pq^{2+}$ has a fluorescence quantum yield in aqueous solution that is near 0 ($<10^{-3}$)[25] and no fluorescence is observed for this ion in clusters of any size. Although Trp fluoresces as a zwitterion in neutral aqueous solution, the fluorescence is quenched at low pH values,[26] i.e., either protonation of Trp or interactions between $TrpH^+$ and $H_3O^+$ induce the quenching of tryptophan fluorescence. Fluorescence does not occur for $TrpH^+(H_2O)_n(g)$ for any of the cluster sizes investigated, which suggests that protonation of Trp quenches the fluorescence of Trp in bulk solution at low pH, as the hydronium ion is not available to quench fluorescence in the nanodrops. Similarly, tyrosine fluoresces in neutral water, but this emission is quenched at low pH.[26] For partially hydrated doubly protonated KYK, any fluorescence resulting from the presence of the tyrosine residue is quenched, potentially by the presence of one or both of the protons that are in close proximity to the tyrosine residue.

These results indicate that only a relatively small number of water molecules are needed for the bulk quantum efficiencies to be reproduced. To our knowledge, the quantum efficiencies of unsolvated ions in the gas-phase have not been measured or reported using more traditional direct fluorescence detection methods, so it is not known exactly how many water molecules are needed to reproduce the bulk quantum efficiencies for these ions, but it appears to be very small (~10 water molecules or fewer). This is in contrast to results for protonated proflavine, for which between 25 and 32 water molecules are required for the bulk quantum efficiency (34%) to be reproduced for $PH^+(H_2O)_n(g)$.[11] For $PH^+(aq)$, internal conversion is very competitive with fluorescence (i.e., the fluorescent quantum yield is much less than 1). Upon removal of water molecules from $PH^+(H_2O)_n$, internal conversion becomes less competitive with fluorescence and the quantum yields dramatically increase. For the ions with quantum yields of ~1, the rate of fluorescence dominates the rate of internal conversion when fully solvated, and thus, any reduced efficiency in the conversion of electronic to vibrational energy that occurs upon removal of water molecules from $M^z(H_2O)_n$ cannot result in an increase in the quantum yield because the yield is already at the maximum possible value of 1. Thus, the quantum efficiencies of ions that fluoresce readily with a quantum yield value of ~1 in bulk solution do not appear to change with decreasing hydration extent of the nanodrops, at least for those containing the ions investigated here.

Interestingly, these data indicate that the presence of $NO_3^-$ in a cluster containing $Ce^{3+}$ (for $n$ ~30) quenches the fluorescence of $Ce^{3+}$ ($CeNO_3^{2+}$ vs $Ce^{3+}$), whereas the presence of $OH^-$ in the $Ce^{3+}$-containing cluster does not (Figure 3). This suggests that there is a specific interaction between $NO_3^-$ and $Ce^{3+}$, which increases the rate of internal conversion between the $S_1$ and $S_0$ states, such that fluorescence is no longer competitive with internal conversion. Thus, the $Ce^{3+}$ and $NO_3^-$ ions in $[Ce^{3+}NO_3^-(H_2O)_n]^{2+}$ clusters for $n$ ~ 30 may not be significantly separated by solvent under these conditions, unlike for $La^{3+}$ and $e^-$ for water clusters with ~30 or more water molecules.[12a] The quenching of $Ce^{3+}(aq)$ fluorescence by the addition of $HNO_3$ was reported by Boden,[27] and this phenomenon was attributed solely to the oxidative conversion of $Ce^{3+}(aq)$ to the nonfluorescent $Ce^{4+}(aq)$. Our nanodrop results suggest that the fluorescent quenching of $Ce^{3+}$ by $HNO_3$ addition could result from the formation of a nonfluorescent contact ion pair between $Ce^{3+}$ and $NO_3^-$.

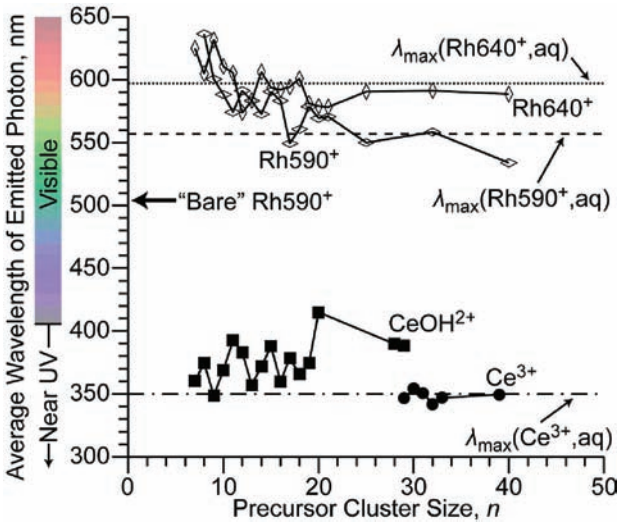


**Figure 4.** Average wavelengths of photons emitted from $M^z(H_2O)_n$, for $M^z$ = $Rh640^+$, $Rh590^+$, $CeOH^{2+}$, and $Ce^{3+}$ upon absorption of a 248 nm photon as a function $n$. Measured fluorescence maxima values, $\lambda_{max}$, from the literature are indicated by dashed lines for the fully solvated ions[28,29] and by the horizontal arrow for fully unsolvated $Rh590^+$.[9h]

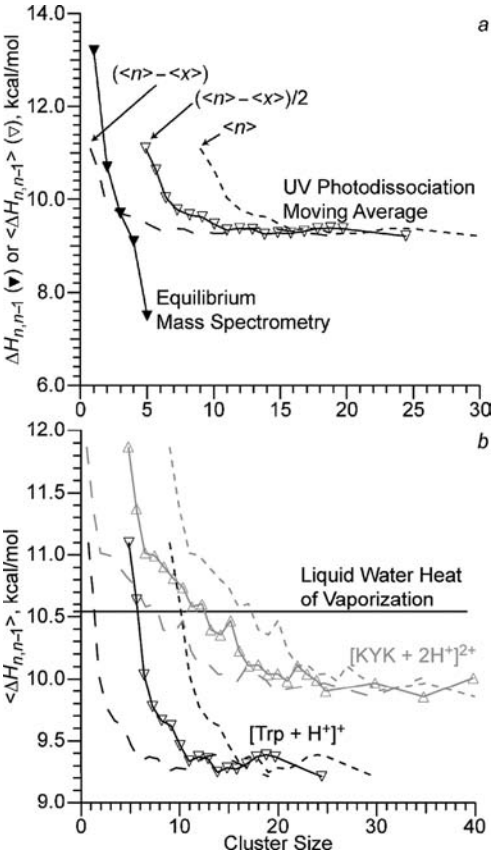


**Figure 5.** (*a*) Average sequential water molecule binding enthalpies, $\langle\Delta H_{n,n-1}\rangle$, of $TrpH^+$ from $\langle n\rangle$ to $(\langle n\rangle - \langle x\rangle)$, obtained from 248 nm photodissociation, as a function of $(\langle n\rangle - \langle x\rangle)/2$ (△), $\langle n\rangle$ (- - -; small dashed lines), and $(\langle n\rangle - \langle x\rangle)$ (— — —; large dashed lines), compared to the sequential water molecule $\Delta H_{n,n-1}$ values measured for individual $TrpH^+(H_2O)_n$ ($n$ = 1−5) from equilibrium mass spectrometry measurements that were reported previously.[18a] (*b*) Average sequential water molecule binding enthalpies for $TrpH^+$ (black lines and symbols) and $[KYK + 2H^+]^{2+}$ (gray lines and symbols), obtained from 248 nm photodissociation, as a function of $(\langle n\rangle - \langle x\rangle)/2$ (solid line and open triangles), $\langle n\rangle$ (small dashed lines), and $(\langle n\rangle - \langle x\rangle)$ (large dashed lines).

**Effects of Cluster Size.** The number of water molecules lost upon absorption of a 248 nm photon also depends on cluster size, in addition to the identity of the ion (Figure 3). For example, $TrpH^+(H_2O)_{n=30}$ loses an average of 10.7 water molecules upon 248 nm photon absorption, whereas the average number of water molecules lost decreases to a value of 8.2 when $n$ = 9. Fewer water molecules are lost with decreasing cluster size in part because water molecule binding energies increase with decreasing cluster size in this size range. In addition, for a fixed amount of internal energy deposition, smaller clusters are heated to higher temperatures than larger clusters, which results in higher $E_{TRV}$ values. At larger sizes, the average number of water molecules lost plateau with increasing cluster size and are essentially independent of cluster size in this size range. For example, $Pq^{2+}(H_2O)_{32}$ loses essentially the same average number of water molecules (∼10.4) as $Pq^{2+}(H_2O)_{80}$. At these larger sizes, both the sequential water molecule binding energies and $E_{TRV}$ values are less dependent on cluster size.[13]

**Average Energy of Photons Emitted from Excited Partially Hydrated Ions.** The average wavelengths of the photons emitted from the partially hydrated laser dyes, $Rh590^+$ and $Rh640^+$, and partially hydrated $Ce^{3+}$ and $CeOH^{2+}$ obtained from the average number of water molecules lost from the cluster as a function of cluster size are shown in Figure 4. The difference between the average wavelengths of emitted photons for the two laser dyes at larger cluster sizes ($n \geq 25$) is 43 ± 11 nm. This value is very close to the difference between the aqueous solution emission maxima of rhodamine 640 and rhodamine 6G (∼40 nm),[28] the latter of which is very closely related to $Rh590^+$ and has the same emission spectra as Rh590 in methanol.[9h] To our knowledge the emission spectra of $Rh590^+(aq)$ has not been reported, but it should be essentially the same as that for rhodamine 6G in water. The average wavelengths of the photons emitted from the partially hydrated rhodamine dyes generally *increase* with decreasing cluster sizes and approach a value of 650 nm for $n$ = 8. A value of 504 nm was measured for the fluorescence emission maxima of unsolvated $Rh590^+(g)$ using direct optical detection of $Rh590^+$ in a quadrupole ion trap.[9h] The interesting red shift away from both the bulk fully hydrated and the "bare" gaseous ion emission maxima (557 and 504 nm, respectively) indicates that the addition of at least 8 water molecules to $Rh590^+(g)$ significantly stabilizes the excited $S_1$ state relative to the ground $S_0$ state, and that the addition of more water molecules from a cluster size of $n$ = 8 to ∼16 leads to a destabilization of the excited state relative to the ground electronic state with increasing cluster size until the bulk value is approached for $n \sim 20$ and larger. These results suggest that the $S_1/S_0$ energy gap does not smoothly transition from the bare gaseous ion to the bulk value with increasing hydration.

Both partially hydrated $Ce^{3+}$ and $CeOH^{2+}$ emit relatively high energy photons. For $Ce^{3+}(H_2O)_n$, $n$ = 30−40, absorption of a 248 nm photon results in emission of a photon with an average wavelength of 348 nm, which is the same as the emission maximum for $Ce^{3+}(aq)$.[29] Addition of $OH^-$ to $Ce^{3+}(H_2O)_n$ clusters results in a 40 nm red shift in the average wavelength of the emitted photon. These results indicate that the wavelengths of

the emitted photons of partially hydrated ions rapidly approach the corresponding condensed-phase value with increasing hydration extent at cluster sizes that are remarkably small (i.e., around 20 or 30 water molecules), and this phenomenon occurs for ions that emit visible (in the case of the laser dyes) as well as UV photons (in the case of $Ce^{3+}$ and $CeOH^{2+}$) via fluorescence.

**Average Water Molecule Binding Energies.** For cluster ions where all the energy of the absorbed 248 nm photon is converted into vibrational energy, the average sequential water molecule binding energies of the lost water molecules can be obtained from the photon energy, the average number of water molecules lost, and the $E_{TRV}$ model.[13] The average sequential water molecule binding enthalpies for $TrpH^+(H_2O)_n$ are shown in Figure 5 as a function of the average cluster size from which water loss occurs, $(\langle n\rangle - \langle x\rangle)/2 = \sim 5$ to 24. With increasing cluster sizes, the average sequential water molecule binding enthalpies decrease from 11.1 kcal/mol for an average cluster size of ~5 and rapidly approach the asymptotic value of ~9.3 kcal/mol for clusters with an average of ~11 or more water molecules. This latter value is lower than the 298 K bulk heat of vaporization of water (10.6 kcal/mol)[30] by 1.3 kcal/mol and lower than the bulk heat of ice sublimation (12.2 kcal/mol)[31] by 2.9 kcal/mol. These results suggest that the structure of water in the nanodrops more closely resembles that of bulk liquid water than ice, which is consistent with UV photodissociation[13] and infrared photodissociation (IRPD)[16] data obtained recently for hydrated metal ions.

Based on the Thomson liquid drop model, surface tension effects on ionic nanodrops can be significant, and lead to a reduction in the sequential water molecule binding energies for clusters relative to the bulk values, but such effects are expected to be largely offset by the presence of the ion in the nanodrop.[20] The gas-phase cluster binding enthalpies may also be lowered due to ion-patterning effects, in which the structure of the water cluster is altered by the presence of the ion vs that for a pure water cluster, and/or via melting point depression, in which the melting point of a material decreases with decreasing size of the material. Bowers and co-workers measured sequential water molecule binding energies to $TrpH^+$ for individual cluster sizes for $n = 1$ to 5 using equilibrium mass spectrometry,[18a] and these values are shown in Figure 5a for comparison with the values obtained using UV photodissociation experiments. The binding enthalpies obtained from equilibrium mass spectrometry rapidly decrease from a value of 13.2 kcal/mol for $n = 1$ to 7.5 kcal/mol for $n = 5$.[18a] The latter enthalpy value is 3.6 kcal/mol lower than the average value obtained for cluster sizes from ~0 to 9 water molecules (11.1 kcal/mol) measured using the UV photodissociation experiments. Although the two data sets are not directly comparable, the average sequential binding enthalpies for clusters with more than $n = 5$ water molecules can be obtained by combining both data sets. For example, the average sequential water molecule binding enthalpy for $n = 6$ to 9 would need to be 12.8 kcal/mol so that the average from $n = 1$ to 9, including the data for $n = 1$ to 5 obtained from equilibrium mass spectrometry measurements, is equal to the average sequential water molecule binding energies measured for $n = \sim 1$ to 9 (11.1 kcal/mol) using the UV photodissociation experiments. An average value for $n = 6$ to 9 of 12.8 kcal/mol is unreasonably high given that the measured value for $n = 1$ is only 13.2 kcal/mol. Furthermore, the average sequential water molecule binding energies smoothly approach a value of 9.3 kcal/mol at larger sizes ($n \geq 11$). Greater oscillation in these values would be expected if binding enthalpies jumped from 7.5 to 12.8 kcal/mol from $n = 5$ to 8. The value of 7.5 kcal/mol obtained for $n = 5$ is also significantly lower than the values obtained at larger sizes. Although it is possible that there is a significant change in the structure of $TrpH^+(H_2O)_n$ clusters upon the addition of several more water molecules to $TrpH^+(H_2O)_5$, it seems more likely that the values obtained from the equilibrium mass spectrometry experiments for at least the larger clusters ($n = 4$ and 5) are aberrantly low.

To further investigate the sequential solvation of biomolecules and the effects of charge on water−water interactions, the average sequential water molecule binding enthalpies for $TrpH^+$ are compared to a doubly protonated tripeptide, $[KYK + 2H^+]^{2+}$, as a function of cluster size in Figure 5b. With increasing cluster sizes, the sequential water molecule binding enthalpies to doubly protonated KYK decrease from a value of 11.9 kcal/mol for an average cluster size of 5 and plateau to a value of ~10.0 kcal/mol for clusters with ~25 water molecules and larger (up to 40 water molecules). The average sequential binding enthalpies are between 0.5 and 1 kcal/mol higher than for $TrpH^+$ for all sizes investigated, consistent with the larger electrostatic potential of the doubly vs singly charged ions. These results indicate that ion identity effects can persist to quite large hydration extents (at least for clusters with ~24 water molecules) and based on the trends in the water molecule binding enthalpies, this persistence appears to continue for much larger clusters as well. IRPD spectroscopy results for hydrated metal ions and the sulfate dianion indicate that ions can pattern water at long distances.[16,32] For example, a free O−H stretch is not observed in IRPD spectra of $SO_4^{2-}(H_2O)_n$, with $n \leq 43$, but a vibrational band corresponding to a free O−H stretch of water molecules at the cluster surface appears at larger cluster sizes,[32] indicating that sulfate can "pattern" water well past the second solvent shell. As is the case for nanodrops containing $TrpH^+$ and divalent metal ions, the asymptotic value for the sequential water molecule binding enthalpies for the doubly charged $[KYK + 2H^+]^{2+}$-containing nanodrops (10.0 kcal/mol) is closer to the bulk heat of liquid water vaporization (10.6 kcal/mol) than that for bulk ice sublimation (12.2 kcal/mol), again suggesting that the structure of water in these droplets more closely resembles that of bulk liquid water than ice.

## CONCLUSIONS

The effects of water on the fluorescence of laser-excited hydrated ions were investigated using an indirect and highly sensitive method for detecting the fluorescence of size-selected nanodrops containing a single fluorescent ion by trapping, isolating, irradiating these ions with 248-nm radiation, and measuring the resulting photodissociation mass spectra. Ions that fluoresce in the bulk with a quantum yield of ~1 such as the laser dyes, $Rh640^+$ and $Rh590^+$, and $Ce^{3+}$ also fluoresce in gas-phase water clusters with the same quantum yield for all cluster sizes investigated ($n$ from 9 to 40), whereas those that do not fluoresce appreciably in bulk do not in the nanodrops, such as paraquat. The energies of the photons emitted from the laser-excited hydrated ions that fluoresce are also close to the bulk photon emission energies for $n = \sim 25$ and larger. Interestingly, the energy of the photons emitted by laser-excited $Rh590^+(H_2O)_n$ do not smoothly progress from that of the bare ion to that in bulk with increasing hydration extent.

For cases in which full internal conversion of the energy of the absorbed UV photon occurs, the average sequential water molecule binding energies can be obtained to investigate the strength of the interactions between solvent molecules and ions. The average sequential water molecule binding enthalpy values for $TrpH^+(H_2O)_n$ and $[KYK + 2H^+]^{2+}(H_2O)_n$ approach respective asymptotic values of ~9.3 ($n \geq 11$) and ~10.0 kcal/mol ($n \geq 25$). These values are near the bulk heat of liquid water vaporization (10.6 kcal/mol), as opposed to the bulk heat of ice sublimation (12.2 kcal/mol), which indicates that the structure of water in these nanodrops more closely resembles bulk liquid water than ice owing to either freezing point depression[33] or kinetic trapping upon rapid evaporative cooling of the initial clusters. Fluorescence does not occur for $TrpH^+(H_2O)_n$ or $[KYK + 2H^+]^{2+}$, presumably because protonation quenches the fluorescence of Trp and the tyrosine residue of KYK, consistent with results for fully hydrated Trp at low pH values. This result suggests that, in bulk solution at low pH values, protonation causes the fluorescence quenching of Trp(aq), as opposed to this effect being caused by interactions between Trp and hydronium ions, as a hydronium ion (or ions) are not available in the nanodrops to quench the fluorescence of Trp. Similarly, nanodrops that contain $Ce^{3+}$ and $CeOH^{2+}$ fluoresce, but those that contain $CeNO_3^{2+}$ do not, indicating that $NO_3^-$ interacts with $Ce^{3+}$ to quench the fluorescence, whereas $OH^-$ does not. These results highlight a major advantage of studying the physical properties of ions in clusters: the composition of the cluster, and therefore, the microenvironment of the ion can be carefully controlled.

This indirect method for detecting the fluorescence of hydrated ions makes it possible to determine the energy of all fluorescent photons irrespective of the direction in which they are emitted, making it equivalent to 100% photon collection efficiency in more traditional fluorescence experiments. This high sensitivity for fluorescence detection should make it feasible to measure FRET in hydrated gaseous ions without any optical detection equipment. Such experiments may provide valuable information about how a controlled number of attached water molecules facilitate the dynamical motions of biomolecules.

## AUTHOR INFORMATION


### Corresponding Author

williams@cchem.berkeley.edu

### Present Addresses

[§]School of Chemistry, Bio21 Institute of Molecular Science and Biotechnology, and ARC Centre of Excellence for Free Radical Chemistry and Biotechnology, University of Melbourne, Australia

[⊥]SRI International, Menlo Park, California, United States


## ACKNOWLEDGMENT

We thank Professor Daniel M. Neumark and Bogdan Negru for the use of, and assistance with, the excimer laser used in these experiments. Financial support was provided by the National Science Foundation (CHE-1012833).

## REFERENCES


(1) (a) Cramer, C. J.; Truhlar, D. G. *Chem. Rev.* **1999**, *99*, 2161. (b) Tomasi, J.; Persico, M. *Chem. Rev.* **1994**, *94*, 2027.

(2) Ludwig, R. *Angew. Chem., Int. Ed.* **2001**, *40*, 1808.

(3) Levy, Y.; Onuchic, J. N. *Annu. Rev. Biophys. Biomol. Struct.* **2006**, *35*, 389.

(4) Zhang, X. X.; Oscarson, J. L.; Izatt, R. M.; Schuck, P. C.; Li, D. *J. Phys. Chem. B* **2000**, *104*, 8598.

(5) (a) Schmidt, J.; Meyer, M. M.; Spector, I.; Kass, S. R. *J. Phys. Chem. A* **2011**, *115*, 7625. (b) Tian, Z.; Kass, S. R. *Angew. Chem., Int. Ed.* **2009**, *48*, 1321.

(6) (a) Prell, J. S.; O'Brien, J. T.; Steill, J. D.; Oomens, J.; Williams, E. R. *J. Am. Chem. Soc.* **2009**, *131*, 11442. (b) Strittmatter, E. F.; Williams, E. R. *J. Phys. Chem. A* **2000**, *104*, 6069. (c) Price, W. D.; Jockusch, R. A.; Williams, E. R. *J. Am. Chem. Soc.* **1997**, *119*, 11988.

(7) (a) Clemmer, D. E.; Jarrold, M. F. *J. Mass Spectrom.* **1997**, *32*, 577. (b) Wyttenbach, T.; Bowers, M. T. *Annu. Rev. Phys. Chem.* **2007**, *58*, 511. (c) Wyttenbach, T.; Bowers, M. T. *Top. Curr. Chem.* **2003**, *225*, 207.

(8) (a) Wu, P. G.; Brand, L. *Anal. Biochem.* **1994**, *218*, 1. (b) Lakowicz, J. R. *Principles of Fluorescence Spectroscopy*; Springer: Singapore, 2006; Vol. 3.

(9) (a) Dashtiev, M.; Azov, V.; Frankevich, V.; Scharfenberg, L.; Zenobi, R. *J. Am. Soc. Mass Spectrom.* **2005**, *16*, 1481. (b) Cage, B.; McFarland, M. A.; Hendrickson, C. L.; Dalal, N. S.; Marshall, A. G. *J. Phys. Chem. A* **2002**, *106*, 10033. (c) Khoury, J. T.; Rodriguez-Cruz, S. E.; Parks, J. H. *J. Am. Soc. Mass Spectrom.* **2002**, *13*, 696. (d) Friedrich, J.; Fu, J. M.; Hendrickson, C. L.; Marshall, A. G.; Wang, Y. S. *Rev. Sci. Instrum.* **2004**, *75*, 4511. (e) Dashtiev, M.; Zenobi, R. *J. Am. Soc. Mass Spectrom.* **2006**, *17*, 855. (f) Sassin, N. A.; Everhart, S. C.; Dangi, B. B.; Ervin, K. M.; Cline, J. I. *J. Am. Soc. Mass Spectrom.* **2009**, *20*, 96. (g) Bian, Q. Z.; Forbes, M. W.; Talbot, F. O.; Jockusch, R. A. *Phys. Chem. Chem. Phys.* **2010**, *12*, 2590. (h) Forbes, M. W.; Jockusch, R. A. *J. Am. Soc. Mass Spectrom.* **2011**, *22*, 93.

(10) (a) Danell, A. S.; Parks, J. H. *Int. J. Mass Spectrom.* **2003**, *229*, 35. (b) Talbot, F. O.; Rullo, A.; Yao, H.; Jockusch, R. A. *J. Am. Chem. Soc.* **2010**, *132*, 16156. (c) Iavarone, A. T.; Patriksson, A.; van der Spoel, D.; Parks, J. H. *J. Am. Chem. Soc.* **2007**, *129*, 6726.

(11) Donald, W. A.; Leib, R. D.; Demireva, M.; Negru, B.; Neumark, D. M.; Williams, E. R. *J. Am. Chem. Soc.* **2010**, *132*, 6904.

(12) (a) Donald, W. A.; Demireva, M.; Leib, R. D.; Aiken, M. J.; Williams, E. R. *J. Am. Chem. Soc.* **2010**, *132*, 4633. (b) Donald, W. A.; Leib, R. D.; Demireva, M.; O'Brien, J. T.; Prell, J. S.; Williams, E. R. *J. Am. Chem. Soc.* **2009**, *131*, 13328. (c) Donald, W. A.; Leib, R. D.; O'Brien, J. T.; Bush, M. F.; Williams, E. R. *J. Am. Chem. Soc.* **2008**, *130*, 3371. (d) Donald, W. A.; Leib, R. D.; O'Brien, J. T.; Williams, E. R. *Chem.—Eur. J.* **2009**, *15*, 5926. (e) Donald, W. A.; Williams, E. R. *J. Am. Soc. Mass Spectrom.* **2010**, *21*, 615. (f) Leib, R. D.; Donald, W. A.; Bush, M. F.; O'Brien, J. T.; Williams, E. R. *J. Am. Chem. Soc.* **2007**, *129*, 4894. (g) Leib, R. D.; Donald, W. A.; Bush, M. F.; O'Brien, J. T.; Williams, E. R. *J. Am. Soc. Mass Spectrom.* **2007**, *18*, 1217. (h) Leib, R. D.; Donald, W. A.; O'Brien, J. T.; Bush, M. F.; Williams, E. R. *J. Am. Chem. Soc.* **2007**, *129*, 7716. (i) Donald, W. A.; Leib, R. D.; O'Brien, J. T.; Holm, A. I. S.; Williams, E. R. *Proc. Natl. Acad. Sci. U.S.A.* **2008**, *105*, 18102. (j) Prell, J. S.; O'Brien, J. T.; Holm, A. I. S.; Leib, R. D.; Donald, W. A.; Williams, E. R. *J. Am. Chem. Soc.* **2008**, *130*, 12680.

(13) Donald, W. A.; Leib, R. D.; Demireva, M.; Negru, B.; Neumark, D. M.; Williams, E. R. *J. Phys. Chem. A* **2011**, *115*, 2.

(14) Bush, M. F.; Saykally, R. J.; Williams, E. R. *J. Am. Chem. Soc.* **2008**, *130*, 9122.

(15) (a) Bush, M. F.; Saykally, R. J.; Williams, E. R. *Chem. Phys. Chem.* **2007**, *8*, 2245. (b) Bush, M. F.; Saykally, R. J.; Williams, E. R. *J. Am. Chem. Soc.* **2008**, *130*, 15482. (c) O'Brien, J. T.; Williams, E. R. *J. Phys. Chem. A* **2008**, *112*, 5893.

(16) Prell, J. S.; O'Brien, J. T.; Williams, E. R. *J. Am. Chem. Soc.* **2011**, *133*, 4810.

(17) (a) Wong, R. L.; Paech, K.; Williams, E. R. *Int. J. Mass Spectrom.* **2004**, *232*, 59. (b) Peschke, M.; Blades, A. T.; Kebarle, P. *J. Phys. Chem. A* **1998**, *102*, 9978. (c) Rodriguez-Cruz, S. E.; Jockusch, R. A.; Williams, E. R. *J. Am. Chem. Soc.* **1998**, *120*, 5842. (d) Rodriguez-Cruz, S. E.; Jockusch, R. A.; Williams, E. R. *J. Am. Chem. Soc.* **1999**, *121*, 8898. (e) Carl, D. R.; Chatterjee, B. K.; Armentrout, P. B. *J. Chem. Phys.* **2010**,

*132*, 044303. (f) Carl, D. R.; Moision, R. M.; Armentrout, P. B. *Int. J. Mass Spectrom.* **2007**, *265*, 308. (g) Cooper, T. E.; Armentrout, P. B. *Chem. Phys. Lett.* **2010**, *486*, 1. (h) Cooper, T. E.; Carl, D. R.; Armentrout, P. B. *J. Phys. Chem. A* **2009**, *113*, 13727.

(18) (a) Gao, B.; Wyttenbach, T.; Bowers, M. T. *J. Am. Chem. Soc.* **2009**, *131*, 4695. (b) Liu, D. F.; Wyttenbach, T.; Barran, P. E.; Bowers, M. T. *J. Am. Chem. Soc.* **2003**, *125*, 8458. (c) Meot-Ner, M.; Field, F. H. *J. Am. Chem. Soc.* **1974**, *96*, 3168. (d) Wyttenbach, T.; Paizs, B.; Barran, P. E.; Breci, L.; Liu, D. F.; Suhai, S.; Wysocki, V. H.; Bowers, M. T. *J. Am. Chem. Soc.* **2003**, *125*, 13768. (e) Liu, D. F.; Wyttenbach, T.; Carpenter, C. J.; Bowers, M. T. *J. Am. Chem. Soc.* **2004**, *126*, 3261. (f) Wincel, H. *Int. J. Mass Spectrom.* **2006**, *251*, 23. (g) Wincel, H. *Chem. Phys. Lett.* **2007**, *439*, 157. (h) Wyttenbach, T.; Liu, D. F.; Bowers, M. T. *Int. J. Mass Spectrom.* **2005**, *240*, 221. (i) Kohtani, M.; Breaux, G. A.; Jarrold, M. F. *J. Am. Chem. Soc.* **2004**, *126*, 1206.

(19) Bush, M. F.; Saykally, R. J.; Williams, E. R. *Int. J. Mass Spectrom.* **2006**, *253*, 256.

(20) Donald, W. A.; Williams, E. R. *J. Phys. Chem. A* **2008**, *112*, 3515.

(21) Klots, C. E. *J. Chem. Phys.* **1985**, *83*, 5854.

(22) (a) Benfey, D. P.; Brown, D. C.; Davis, S. J.; Piper, L. G.; Foutter, R. F. *Appl. Opt.* **1992**, *31*, 7034. (b) Kubin, R. F.; Fletcher, A. N. *J. Lumin.* **1982**, *27*, 455. (c) Magde, D.; Rojas, G. E.; Seybold, P. G. *Photochem. Photobiol.* **1999**, *70*, 737.

(23) Klán, P.; Wirz, J. *Photochemistry of Organic Compounds: From Concepts to Practice*; Wiley: Chippenham, Wiltshire, 2009.

(24) (a) Karstens, T.; Kobs, K. *J. Phys. Chem.* **1980**, *84*, 1871. (b) Kaizu, Y.; Miyakawa, K.; Okada, K.; Kobayashi, H.; Sumitani, M.; Yoshihara, K. *J. Am. Chem. Soc.* **1985**, *107*, 2622.

(25) (a) Villemure, G.; Detellier, C.; Szabo, A. G. *J. Am. Chem. Soc.* **1986**, *108*, 4658. (b) Villemure, G.; Detellier, C.; Szabo, A. G. *Langmuir* **1991**, *7*, 1215.

(26) White, A. *Biochem. J.* **1959**, *71*, 217.

(27) Boden, H. *Nature* **1969**, *222*, 161.

(28) (a) Sutton, J. A.; Fisher, B. T.; Fleming, J. W. *Exp. Fluids* **2008**, *45*, 869. (b) Yaginuma, N.; Hirose, S.; Inada, Y. *J. Biochem.* **1973**, *74*, 811.

(29) Kirkbright, G. F.; West, T. S.; Woodward, C. *Anal. Chim. Acta* **1966**, *36*, 298.

(30) Marsh, K. N. *Recommended Reference Materials for the Realization of Physiochemical Properties*; Oxford: Blackwell, 1987.

(31) Feistel, R.; Wagner, W. *J. Phys. Chem. Ref. Data* **2006**, *35*, 1021.

(32) O'Brien, J. T.; Prell, J. S.; Bush, M. F.; Williams, E. R. *J. Am. Chem. Soc.* **2010**, *132*, 8248.

(33) (a) Hock, C.; Schmidt, M.; Kuhnen, R.; Bartels, C.; Ma, L.; Haberland, H.; von Issendorff, B. *Phys. Rev. Lett.* **2009**, *103*, 073401. (b) Schmidt, M.; Kusche, R.; Kronmuller, W.; von Issendorff, B.; Haberland, H. *Phys. Rev. Lett.* **1997**, *79*, 99.